National Aeronautics and Space Administration

Computational Modeling of Cephalad Fluid Shift for Application to Microgravity-Induced Visual Impairment

E.S. Nelson,[1] L. Best,[1] J.G. Myers,[1] and L. Mulugeta[2]
[1]NASA Glenn Research Center, Cleveland, Ohio, [2]Universities Space Research Association, Houston, Texas

Introduction

An improved understanding of spaceflight-induced ocular pathology is of keen interest to space medicine. Cephalad fluid shift causes a profoundly altered distribution of fluid within the compartments of the head and body, and may indirectly generate phenomena that are biomechanically relevant to visual acuity. On Earth, elevated intracranial pressure (ICP) is a key element in the diagnosis of idiopathic intracranial hypertension (IIH), which can produce ocular pathologies that look similar to those seen in some astronauts returning from long-duration flight. However, the clinically observable features of the Visual Impairment and Intracranial Pressure (VIIP) syndrome in space and IIH on Earth are not entirely consistent. Moreover, there are at present no experimental measurements of ICP in microgravity (μg). By its very nature, physiological measurements in spaceflight are sparse, and the space environment does not lend itself to well-controlled experiments. In the absence of such data, numerical modeling can play a role in the investigation of biomechanical causal pathways that are suspected of involvement in VIIP. In this work, we describe the conceptual framework for modeling the altered compartmental fluid distribution that represents an equilibrium fluid distribution resulting from the loss of hydrostatic pressure.

Lumped Parameter (LP) Approach to Cephalad Fluid Shift

The fluid in the body can arbitrarily be represented by 3 compartments, with compartmental compliance, C(p, V), which is dependent on pressure p and volume V, and resistance to flux between compartments, R(d, …), which is a function of vessel diameter, d, and other parameters. In 1g, the hydrostatic pressure is ρgh, where ρ is the fluid density, g is gravitational acceleration and h is the mean fluid height in the compartment, shown in Fig. 1(a). At equilibrium, no fluid flux (in the mean) exists between compartments. Upon entry to μg, the hydrostatic pressure is transferred into an elastic force (Fig. 1(b)) that propels fluid headwards. Once the gross fluid redistribution is established, the body seeks a compartmental equilibrium, shown in Fig. 1(c). During space adaptation, the spine elongates, the lower extremities maintain a fluid deficit while the torso and head exhibit bulk fluid increase, and the center of mass moves headwards. The adaptation process is mediated by a range of regulatory responses.

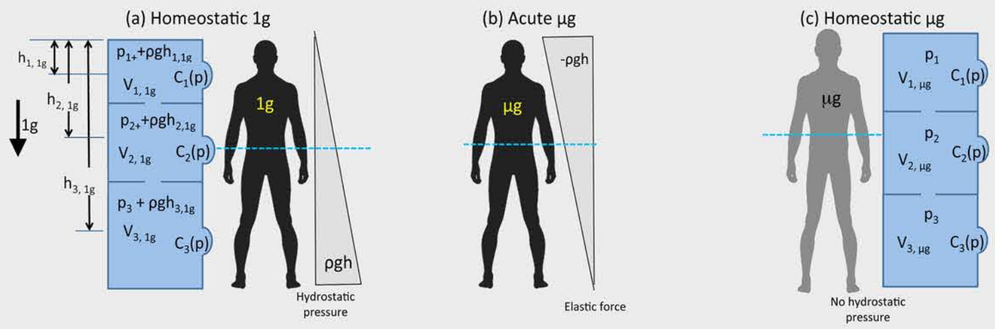

Figure 1. LP parameter representation of fluid distribution in 1g and μg.

Clinical observations of astronauts affected by VIIP indicate that symptoms appear at 3 weeks to 3 months into flight. One numerical approach would be to simulate fluid redistribution chronologically from Fig. 1(a) through (b) to (c). However, we can simplify the problem by skipping directly over the acute response in (b). If we understand the dependence of compliance and resistance on pressure, calculating the base homeostatic state in 1g is straightforward. The appropriate definition of tissue properties thus becomes the one of the most important steps in minimizing uncertainty in the numerical model.

We hypothesize that the equilibrium fluid distribution in μg is the key to understanding the biomechanical conditions that contribute to VIIP. We can simplify the problem and avoid uncertainties in modeling the regulatory functions by skipping directly from the homeostatic base state at 1g in (a) to that of μg in (c).

System Level Model of Fluid Pathways

Figure 2 presents an integrated, open-loop, whole-body system of fluid pathways for transport among the cardiovascular system (CVS), the central nervous system (CNS), and the lymphatic system (LS).

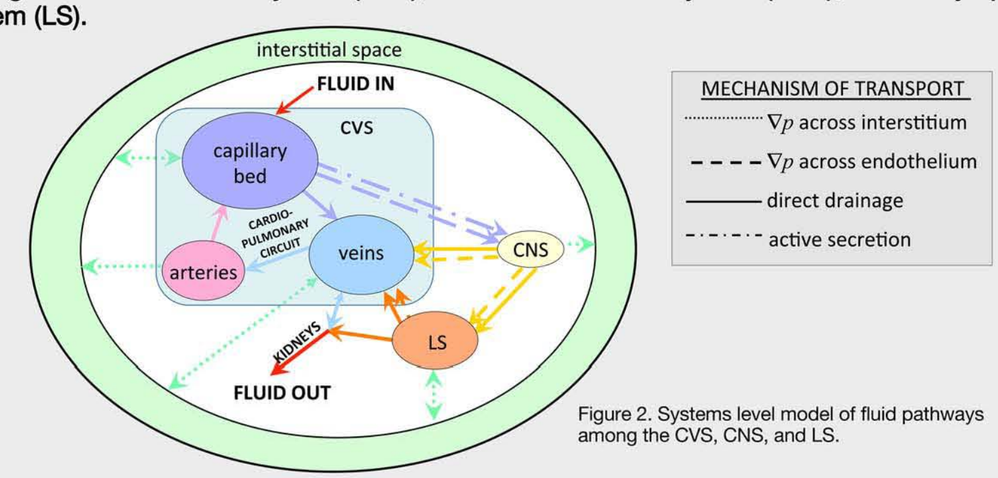

Figure 2. Systems level model of fluid pathways among the CVS, CNS, and LS.

The CVS is described in Fig. 2 by three compartments representing the arterial and venous systems and the capillary bed. Additional compartments for the CVS could be added, depending on the problem of interest. Fluid transport between systems can be driven by active secretion, direct drainage, or pressure gradients, typically across porous interfaces between compartments. Oncotic pressure between systems may vary due to intercompartmental compositional variations. In addition to this system-level description, spatial resolution must be added to capture the effect of hydrostatic pressure loss. For the case of the CVS, a minimal increase in resolution could be obtained by splitting each of its three system-level compartments (arterial,venous, and capillary) into three spatial subcompartments, as in Fig. 1, to permit some discrimination of the effects of hydrostatic pressure gradient.

The CVS, CNS, and LS can be integrated into a single model. These systems are connected by fluid flow across the interstitial space and other pathways as marked.

Integration Strategy

A spatially resolved model (Fig. 3(a)), such as a finite element model, is needed to explore the detailed biomechanical state of the sclera, choroid, optic nerve head, and the retrobulbar space. This module communicates with a tissue remodeling algorithm through the tissue stress, σ, and strain, ε to evolve tissue properties in time. Boundary conditions for Fig. 3(a) are obtained from Figs. 3(b) and (c). The whole-body LP model in Fig. 3(c) can be queried to obtain fluid flow rate, Q, and pressure, P, associated with any compartment. It supplies ICP from the CNS model and the arterial and venous flow into the cranial space from the CVS model, which is related to the blood flows entering and leaving the tissues of the eye. In turn, the eye LP model (b) uses these boundary conditions, along with a model for aqueous flow, to calculate IOP.

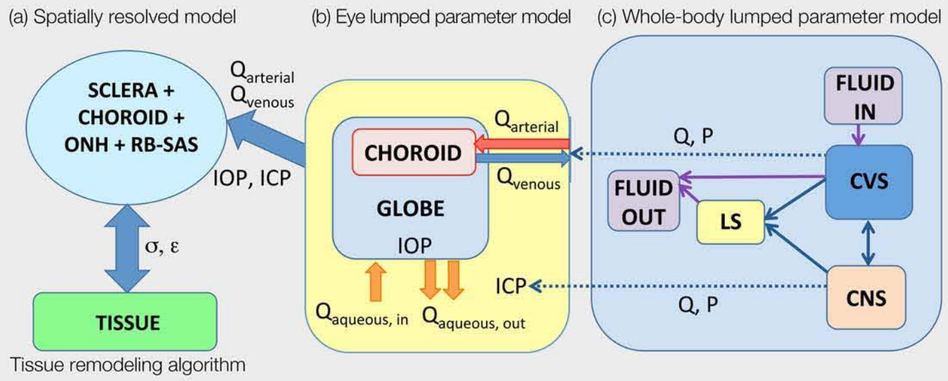

Figure 3. Relationship among lumped parameter and spatially resolved models.

The LP models in Figs. 3(b) and (c) can identify the criticality of parameters on mean ICP and IOP in μg, including those associated with vascular congestion, choroidal engorgement and altered translaminar pressure gradient. Time-dependent simulations can examine peak ICP during exercise.

Conclusions

We have presented a consistent conceptual framework for a set of lumped-parameter models to calculate mean ICP, IOP, and blood flows to the tissues of the eye. By taking advantage of the physical principles that drive equilibrium fluid distribution in μg, this approach simplifies the task of computing the compartmental fluid distributions by directly calculating the homeostatic state in μg. These models can then be used to study the relative importance of various biomechanical pathways on ICP and IOP. The data from this model can be used to drive a spatially resolved numerical model of the globe and surrounding tissues to investigate the potential for globe flattening, optic disk edema, and distension of the optic nerve and its sheath.